JOC The Journal of Organic Chemistry

Note

Four-component Domino Synthesis of Pyrazolo[3,4-*h*]quinoline-3-carbonitriles: 'Turn-off' Fluorescent Chemosensor for Fe Ions

Adaikalam Shylaja, Somi Santharam Roja, Rakkappan Vishnu Priya, and Raju Ranjith Kumar

J. Org. Chem., **Just Accepted Manuscript** • DOI: 10.1021/acs.joc.8b01991 • Publication Date (Web): 25 Oct 2018

Four-component Domino Synthesis of Pyrazolo[3,4-*h*]quinoline-3-carbonitriles: 'Turn-off' Fluorescent Chemosensor for Fe^{3+} Ions

Adaikalam Shylaja,[†] Somi Santharam Roja,[†] Rakkappan Vishnu Priya[‡] and Raju Ranjith Kumar*[,†]

[†]Department of Organic Chemistry, School of Chemistry, Madurai Kamaraj University, Madurai 625021, Tamil Nadu, INDIA.

[‡]Department of Physics, Madura College, Madurai 625011, Tamil Nadu, INDIA.

Abstract

The synthesis of novel pyrazolo[3,4-*h*]quinoline-3-carbonitriles has been achieved through a one-pot, four-component domino strategy under solvent-free microwave conditions. One of these compounds exhibited fluorescence under UV lamp and was found to be highly sensitive towards Fe^{3+} ions in DMSO against various metal ions with a detection limit of 8.6×10^{-7} M.

Keywords: Domino reaction; pyrazolo[3,4-*h*]quinolone; Microwave-assisted; Fluorescence; Chemosensor; Iron.

Iron is one of the most abundant and multifaceted elements and an integral part of all the living systems. It is an essential trace element in the biological processes like oxygen metabolism, electron transfer and transcriptional regulation.[1,2] Deficiency of iron results in anemia, whereas an excess in the level may lead to hepatitis, certain cancers and deterioration of vital organs[3–6] apart from causing Alzheimer's and Parkinson's diseases.[7] Hence proper attention in monitoring the level of iron is imperative. Complexity in the operation of existing techniques mandates the development of simple and cost effective methodologies for detecting iron.[6–8] The spectrofluorometric technique employing fluorescence materials is one of the versatile methods for the detection of heavy metal ions including iron.[9] This methodology has been widely used for sensing and imaging in chemical and medical fields.[10–13] Several Fe^{3+} based fluorescence chemosensors exhibiting both "turn-off" and "turn-on" mechanisms have been reported.[13–22] However, incessant effort is being continually put towards the design and development of cost-effective, highly selective and sensitive fluorescent probes for the detection of Fe^{3+} ions.

Pyrazoloquinolines are privileged class of organic heterocycles possessing broad array of applications,[23] for example, in materials chemistry as electroluminescent materials, light emitting diodes and fluorescent chemosensors.[24] In addition pyrazoloquinolines display antiviral, antibacterial, anti-proliferative and immunosuppressant activities apart from exhibiting oral antipsychotic activity in the MK-801 induced hyperactive rat model.[25] Among the pyrazoloquinolines, the syntheses and applications of pyrazolo[3,4-*b*]quinolone derivatives have been investigated extensively.[23–26] However, the syntheses of pyrazolo[3,4-*h*]quinolines have received less attention.[27] In the present work novel pyrazolo[3,4-*h*]quinoline-3-carbonitriles have been synthesized through a one-pot, four-component domino strategy under microwave conditions. Incidentally, multi-component domino reactions (MDRs) are environmentally benign

protocols widely employed to synthesize natural and unnatural compounds of biological importance.[28] On the other hand microwave-assisted reactions are energy efficient process that offers a simple and rapid access to complex molecules.[29] Microwave-assisted MDRs further augment the greenness of the reaction towards sustainable chemical synthesis.[30]

Initially, the precursor 1-aryl-1,5,6,7-tetrahydro-4*H*-indazol-4-ones **1** were synthesized following literature procedure (**Table 1**).[31] Subsequently the reaction of 1-phenyl-1,5,6,7-tetrahydro-4*H*-indazol-4-one **1**, 4-chlorobenzaldehyde **2a**, malononitrile **3** and ammonium acetate **4** presumably affording pyrazolo[3,4-*h*]quinoline-3-carbonitrile **5a** was taken as a model in order to find out the optimized reaction condition (**Table 1**). To begin with an equimolar mixture of the above reactants was refluxed in ethanol, which afforded **5a** in 50% after 6 h. The yield of **5a** increased to 70% when two equivalent of ammonium acetate was employed. This reaction in refluxing acetic acid afforded 80% of **5a**, whereas a neat mixture of the above reactants at 100°C yielded 75% of **5a** after 6h.

Table 1. Optimization of the reaction condition

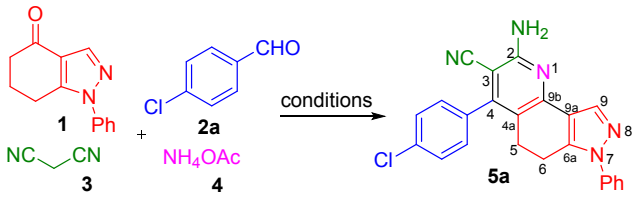

Entry	Condition	Yield of **5a** (%)[a]
1	Ethanol, reflux, 6h	50
2	Ethanol, reflux, 6h (with 2 equiv. of **4**)	70
3	Acetic acid, reflux, 6h	80
4	Solvent-free, 100°C, 6h	75
5	Microwave, 2–3 min	96

[a]Isolated yield

Gratified with the yield of **5a** obtained under solvent-free conditions, we explored to perform the above reaction under solvent-free microwave heating. Accordingly, a 1:1:1:2 mixture of **1**, **2a**, **3** and **4** was taken in a microwave vial and mixed thoroughly. Then the closed vail was irradiated at 110°C in a microwave synthesizer. The progress of the reaction was monitored by TLC after every 1 min of irradiation, which revealed the reaction completed within 2–3 min. The mixture was then cooled to room temperature and 2 mL of ethanol was added. The precipitate formed was filtered, washed with ethanol (2 mL) and dried under vacuum to obtain pyrazolo[3,4-*h*]quinoline-3-carbonitrile **5a** in 96% yield. The structure of **5a** was elucidated unambiguously using NMR spectroscopy and further confirmed from single crystal X-ray studies (**Figure S9**, SI).[32] The optimized condition was then employed to synthesize nine novel pyrazolo[3,4-*h*]quinoline-3-carbonitriles **5a–i** in 88–96% yields (**Scheme 1**). In addition, two isomeric products **5j** and **5k** were isolated when the reaction was performed with ethyl cyanoacetate instead of malononitrile.

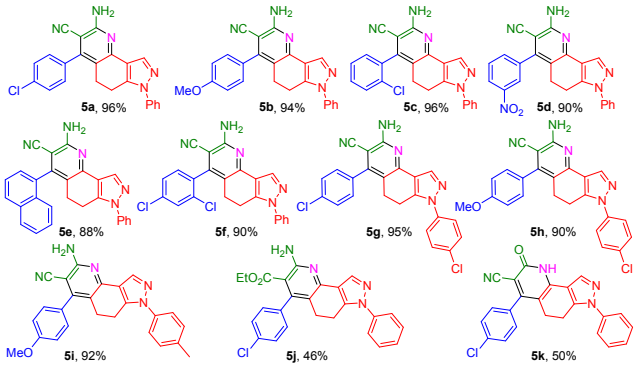

Scheme 1. Pyrazolo[3,4-*h*]quinoline derivatives **5a–k**

The plausible mechanism for the formation of pyrazolo[3,4-*h*]quinoline-3-carbonitriles **5** is given in **Scheme 2**. The Knoevenagel condensation of aromatic aldehyde **2** and malononitrile **3** affords 2-arylidenemalononitrile **6**, which undergoes Michael addition with tetrahydro-4*H*-

indazol-4-one **1** to form the ketenimine intermediate **7**. The nucleophilic addition of ammonium acetate **4** to the carbonyl of **7** leads to the formation of enamine **8**. The enamine intermediate **8** undergoes intramolecular *N*-cyclization to afford the pyrazolo[3,4-*h*]quinoline-3-carbonitrile **9**, which upon oxidative aromatization by molecular oxygen as the sole oxidant affords the pyrazolo[3,4-*h*]quinoline-3-carbonitriles **5**. This multi-step domino reaction leads to the formation of two new C–C and C–N bonds in a single transformation affording the products **5a–i** in excellent yields.

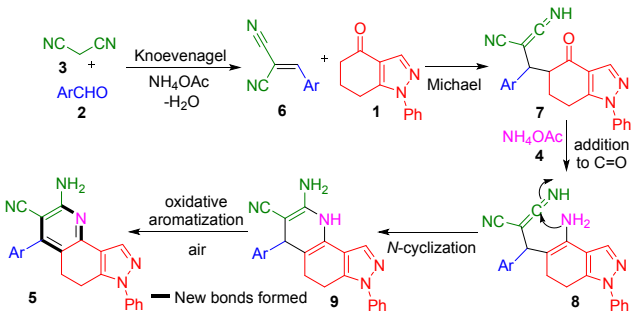

Scheme 2. Plausible mechanism for the formation of **5**

Among the pyrazolo[3,4-*h*]quinoline-3-carbonitriles, compounds **5a–c**, **5e** and **5g** exhibited blue fluorescence under UV lamp. The relative quantum yield of **5** was measured using anthracene in ethanol as standard (**Table S2**, SI).[33] The pyrazolo[3,4-*h*]quinoline-3-carbonitrile **5b** was chosen for further studies in view of its higher quantum yield of 0.60. The initial solvatochromism studies of **5b** in chloroform, methanol, ethyl acetate, DMSO, DCM and THF (20 μM each) revealed notable red shift in the UV absorption of **5b** in DMSO and methanol (**Table S3**, SI). The maximum absorption of **5b** in DMSO (20 μM) was found to be around 370 nm, which may be attributed to the π–π* or n–π* transitions. The fluorescence emission

spectrum of **5b** was recorded in DMSO (20 μM) with an excitation wavelength of 370 nm and maximum fluorescence emission intensity was observed at 415 nm (**Figures S33–S36**, SI).

Subsequently, changes in the absorption and fluorescence response of the probe **5b** in DMSO (20 μM) at an excitation/emission wavelengths of 370/415 nm towards thirteen different metal ions namely Ag^{+}, Al^{3+}, Ba^{2+}, Co^{2+}, Cr^{3+}, Cu^{2+}, Fe^{2+}, Fe^{3+}, Hg^{2+}, Na^{+}, Ni^{2+}, Pb^{2+} and Zn^{2+} (in water, 2×10^{-4} M) at room temperature was investigated. No major changes in the UV absorption was noted upon the addition of Ag^{+}, Al^{3+}, Ba^{2+}, Co^{2+}, Cr^{3+}, Fe^{2+}, Hg^{2+}, Na^{+}, Ni^{2+}, Pb^{2+} or Zn^{2+} to the probe solution. However, significant blue shift to 356 and 283 nm was observed upon addition of $Fe^{3+}$and Cu^{2+}, respectively (**Figure 1**). Similarly the changes in the fluorescence spectra of **5b** were observed upon addition of the above metal ions to the probe solution. It is pertinent to note that the fluorescence intensity of the probe **5b** significantly quenched upon adding Fe^{3+} (**Figure 2**).

Further, the UV and emission spectra of probe **5b** with various concentration of Fe^{3+} ranging from 0 to 500 μM showed linear relationships while plotting absorbance/fluorescence vs concentration of Fe^{3+}. These observations reveal that probe **5b** is suitable for detecting Fe^{3+}. From the Stern-Volmer plot the Stern-Volmer constant (K_{sv}) was found to be 1.5×10^{4} M^{-1}, which linearly decreased with a regression coefficient of 0.983. The lower limit of detection (LOD) was found to be 8.6×10^{-7} M. In addition, the stoichiometry binding ratio of probe **5b** with Fe^{3+} ion was calculated as 1:1 from the Job's plot (**Figures S37**–**S40**, SI).

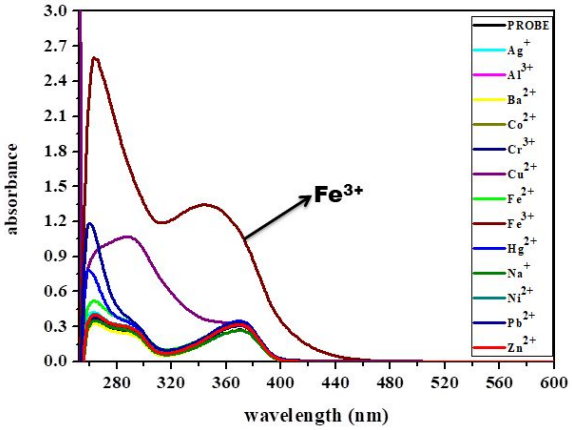

Figure 1. UV spectra of **5b** in the presence of various metal ions

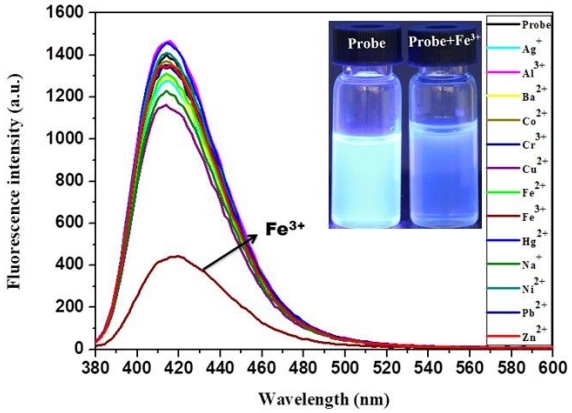

Figure 2. Emission spectra of **5b** in the presence of various metal ions

To establish the selectivity of probe **5b** towards Fe^{3+} over a range of metal ions, competitive experiments were carried out with high concentration of other metal ions *viz*. Ag^{+}, Al^{3+}, Ba^{2+}, Co^{2+}, Cr^{3+}, Cu^{2+}, Fe^{2+}, Hg^{2+}, Na^{+}, Ni^{2+}, Pb^{2+} and Zn^{2+} (10 equiv.). The presence of other metal ions had no effect on the quenching intensity and hence it is clear that the probe **5b** is selective towards Fe^{3+}. However, interference was observed in the case of Cr^{3+}.[34–38]

The probe **5b** was compared with various other probes from the literature (**Table S4**, SI) for relative quantum yield and LOD. From the table it is clear that the probe **5b** has high

quantum yield of 0.60 when compared to the probes listed and highly sensitive towards Fe^{3+} with LOD of 8.6×10^{-7} M, which is in good agreement with the probes already reported.

In order to gain insight into the quenching mechanism, theoretical calculations of **5b** and **5b+Fe^{3+}** were performed at DFT using Gaussian 09 program. The structure of **5b** and **5b+Fe^{3+}** was optimized using B3LYP and B3LYP/LanL2DZ basis set, respectively (**Figure 3**).[39] The frontier molecular orbital analysis reveals that in probe **5b** HOMO is located over pyrazolo[3,4-*h*]quinoline unit, the amino and cyano groups, whereas the LUMO is spread over the whole molecule. However, in **5b+Fe^{3+}** HOMO appears mainly over the pyridine ring and the amino group, whereas the LUMO is located over Iron (**Figure 3**). Further, the calculated HOMO-LUMO energy gap difference for **5b+Fe^{3+}** (3.0453 eV) is lesser than that of the probe **5b** (4.0379 eV), which also indicates favorable coordination between the probe **5b** and Fe^{3+}. From the above observations it can be concluded that an internal charge transfer (ICT) occurs between the electron-releasing methoxy group in the phenyl ring and the electron withdrawing CN group in the pyrazolo[3,4-*h*]quinoline ring, which induces fluorescence turn on in the probe **5b**. The complexation of the probe **5b** with Fe^{3+} inhibits the ICT and hence results in fluorescence turn off.

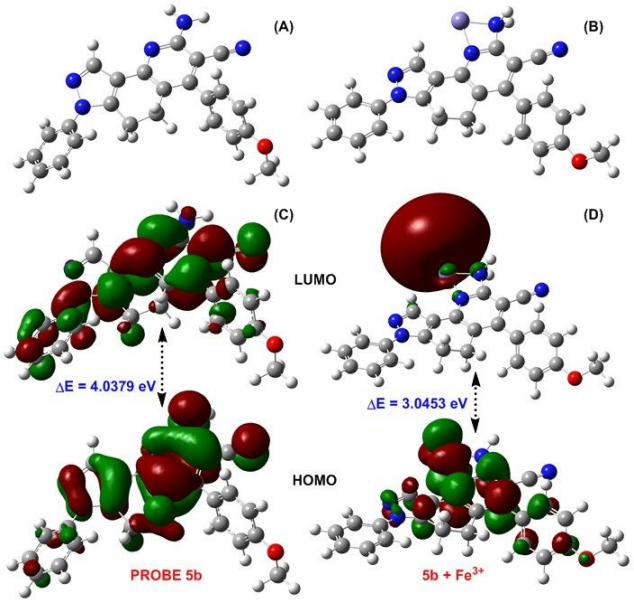

Figure 3. Optimized structure of (A) **5b** and (B) **5b+Fe^{3+}**. Frontier molecular orbital of (C) probe **5b** and (D) **5b+Fe^{3+}**

To further vindicate the quenching mechanism, the fluorescence lifetime measurements were recorded for the probe **5b** (20 μM) and **5b+Fe^{3+}** (20 μM **5b** + 200 μM Fe^{3+}) using time-correlated single photon counting spectrometer (**Figure S60** and **Table S5**, SI). The average fluorescence lifetime (τ) of the probe **5b** and the complex **5b+Fe^{3+}** was found to be 0.24 and 0.23 ns, respectively. The results indicate that the fluorescence decay profiles of **5b** and **5b+Fe^{3+}** remain unchanged and hence the quenching mode is static.

With a view to study the practical applicability of probe **5b**, real sample analyses was performed to determine the concentration of Fe^{3+} in three different water samples. Drinking water (reverse osmosis treated) from the authors department, river water from Thamirabarani at Tirunelveli and tap water from Velachery, Chennai was collected, filtered and used for the analysis (**Table S6** and **Figures S61**, SI). The water samples were spiked with standard Fe^{3+} at three different concentrations and determined by standard addition method using the probe **5b**. Emission studies were performed by taking 40 μl of **5b** from 10^{-3} M stock solution in 2 mL

DMSO with corresponding 30, 40 and 50 μl Fe^{3+} spiked water samples from 10^{-2} M solution (0.0162 g in 10 mL of water sample). The average recovery of the spiked samples was found to be 109, 94 and 117 respectively for drinking, tap and river water samples. The results show that the probe **5b** successfully quantifies the amount of Fe^{3+} in the water samples.

Conclusions

In conclusion, novel pyrazolo[3,4-*h*]quinoline-3-carbonitriles **5a–i** were synthesized through a facile one-pot, four-component reaction of 1-aryl-1,5,6,7-tetrahydro-4*H*-indazol-4-ones, aromatic aldehydes, malononitrile and ammonium acetate under environmentally benign solvent-free microwave conditions. The reaction presumably occurred via domino Knoevenagel condensation–nucleophilic addition–Michael addition–intramolecular *N*-cyclization–oxidative aromatization sequence of reactions in a single transformation affording the pyrazolo[3,4-*h*]quinoline-3-carbonitriles **5a–i** in excellent yields. Among the synthesized compounds the pyrazolo[3,4-*h*]quinoline-3-carbonitrile **5b** exhibited fluorescence in UV and was able to sense Fe^{3+} ions through "turn off" mechanism with a detection limit of 8.6×10^{-7} M in DMSO.

EXPERIMENTAL SECTION

General information

The melting points were measured in open capillary tubes and are uncorrected. The microwave reactions were performed in CEM DISCOVER, Benchmate model single-mode design. The reaction temperature was monitored with an inbuilt floor mounted IR sensor. The ^{1}H, $^{13}C\{^{1}H\}$ and 2D NMR spectra were recorded on Bruker (Avance) 300 MHz or (Avance III HD Nanobay) 400 MHz NMR instruments using TMS as internal standard and $CDCl_3$ or

$CDCl_3$+DMSO mixture as solvents. Standard Bruker software was used throughout. Chemical shifts are given in parts per million (δ-scale) and the coupling constants are given in Hertz. The UV–vis spectrum of the sample was measured using JASCO (v-630) spectrophotometer. The Photoluminescence (PL) spectra were acquired using JASCO (F-8500) fluorescence spectrophotometer. Sample was placed in a 3 mL quartz cuvette to get PL spectra. The PL experiments were run in proper wavelength window with 0.2 nm steps. The PMT voltage was set to auto. The time-resolved fluorescence life time measurements were carried out using time-correlated single photon counting (TCSPC) spectrometer, Edinburgh instrument FLS 980 model (UK). HR-Mass data were recorded on Agilent Accurate-Mass Q-TOF (model HAB 273). The IR data were recorded in NICOLET 6700 ATR-FT-IR instrument. The single crystal X-ray data were collected on Enraf–Nonius (CAD4) diffractometer with Mo Kα (λ=0.71073 Å) radiation. Scan range was $2.02^o \leq \theta \leq 24.97^o$. SHELXTL software was used for structure solution and refinement. Silica gel-G plates (Merck) were used for TLC analysis with a mixture of petroleum ether (60–80^{o}C) and ethyl acetate as eluent. All the chemicals were purchased from Sigma-Aldrich and used without any further purification. The ground-state geometries were optimized using density functional theory with B3LYP and LANL2DZ hybrid functional at the basis set level of 6-31/6-311G*. All the calculations were performed using Gaussian 09 package.

UV-vis and Photoluminescence (PL) experiments

The stock solution (10^{-3} M) of the probe was prepared by taking 0.0012 g of **5b** in 3 mL DMSO. The stock solution of the Fe^{3+} ions was prepared by taking 0.016 g of Iron (III) chloride in 10 mL double distilled water. Then 20 μM of sample **5b** from the stock solution was placed in a quartz cuvette to get absorbance and PL spectra using the respective instruments. The PL experiments of Fe^{3+} ions determination was carried out by adding 2×10^{-4} M of Fe^{3+} from 10^{-2}

M stock solution added to the probe. The excitation wavelength for this experiment is 370 nm. The PL experiments for interference studies were run in the same excitation wavelength and emission intensities recorded at wavelength of 415 nm. All metal ion solutions were prepared in Double Distilled (DD) Water from the corresponding metal chloride salts and used for metal interference studies. For all the fluorescence measurements, the excitation/emission wavelengths are set to 370/415 nm under room temperature.

General procedure for the synthesis of 1-aryl-1,5,6,7-tetrahydro-4*H*-indazol-4-ones 1

2-((Dimethylamino)methylene)cyclohexane-1,3-dione (1 mmol) and aryl hydrazine (1 mmol) in water (1 mL) were mixed thoroughly in a microwave vial followed by addition of glacial acetic acid (1 mmol). The closed vial was subjected to irradiation in a microwave synthesizer (CEM DISCOVER, Benchmate model, single-mode design with inbuilt IR temperature sensor) for 2 minutes at 200 ^{o}C. Then the microwave vial was cooled to room temperature and 6–7 mL of water was added. The resultant precipitate was filtered and dried to obtain the 1-aryl-1,5,6,7-tetrahydro-4*H*-indazol-4-ones **1**, which was used for subsequent reactions.

General procedure for the synthesis of pyrazolo[3,4-*h*]quinoline derivatives 5a–k

A mixture of 1-aryl-1,5,6,7-tetrahydro-4*H*-indazol-4-ones **1**, (1 mmol), aromatic aldehydes **2**, (1 mmol), malononitrile/ethyl cyanoacetate **3**, (1 mmol) and ammonium acetate **4**, (2 mmol) was taken in a microwave vail and mixed thoroughly. The closed vial was then irradiated at 110^{o}C in a microwave synthesizer (CEM DISCOVER, Benchmate model, single-mode design with inbuilt IR temperature sensor). The progress of the reaction was monitored by TLC after every 1 min of irradiation, which revealed the reaction completed within 2–3 min. The mixture was cooled to room temperature and 2 mL of ethanol was added. The precipitate formed

was filtered, washed with ethanol (2 mL) and dried under vacuum to obtain pyrazolo[3,4-*h*]quinoline derivatives **5**.

2-Amino-4-(4-cholorophenyl)-7-diphenyl-6,7-dihydro-5H-pyrazolo[3,4-h]quinoline-3-carbonitrile **5a**. Obtained as yellow solid; Yield: 0.179g, 96%; m.p.: 250–253 °C; IR ν: 3323, 2199, 1740, 1549, 1505 cm^{-1}; ^1H NMR (300 MHz, $CDCl_3$) δ 8.21 (s, 1H), 7.25–7.50 (m, 9H), 5.25 (s, 2H), 2.94 (t, *J*=6.0 Hz, 2H), 2.73 (t, *J*=6.0 Hz, 2H); $^{13}C\{^1H\}$ NMR (75 MHz, $CDCl_3$) δ 159.1, 153.8, 151.6, 143.1, 139.3, 138.1, 135.7, 135.0, 130.2, 129.7, 129.5, 128.2, 123.7, 120.3,117.3, 116.6, 88.4, 25.7, 21.9. HRMS (ESI-TOF) m/z: $[M + H]^+$ Calcd for $C_{23}H_{17}ClN_5$ 398.1172; Found 398.1162.

2-Amino-4-(4-methoxyphenyl)-7-diphenyl-6,7-dihydro-5H-pyrazolo[3,4-h]quinoline-3-carbonitrile **5b**. Obtained as yellow solid; Yield: 0.174 g, 94%; m.p.: 260–263 °C; IR ν: 3331, 2202, 1739, 1554, 1502 cm^{-1}; ^1H NMR (300 MHz, $CDCl_3$) δ 8.20 (s, 1H), 7.38–7.50 (m, 4H), 7.37–7.43 (m, 1H), 7.23–7.32 (m, 3H), 7.02 (d, *J*=9.0 Hz, 2H), 5.19 (s, 2H), 3.87 (s, 3H), 2.90 (t, *J*=6.0 Hz, 2H), 2.70 (t, *J*=6.0 Hz, 2H); $^{13}C\{^1H\}$ NMR (75 MHz, $CDCl_3$) δ 160.5, 159.2, 153.5, 152.8, 143.2, 139.3, 138.1, 130.2, 129.8, 128.7, 128.1, 123.7, 120.5, 117.9, 116.9, 114.5, 89.0, 55.8, 25.7, 21.9. HRMS (ESI-TOF) m/z: $[M + H]^+$ Calcd for $C_{24}H_{20}N_5O$ 394.1668; Found 394.1661.

2-Amino-4-(2-cholorophenyl)-7-diphenyl-6,7-dihydro-5H-pyrazolo[3,4-h]quinoline-3-carbonitrile **5c**. Obtained as yellow solid; Yield: 0.179 g, 96%; m.p.: 275–278 °C; IR ν: 3353, 2209, 1740, 1557, 1505 cm^{-1}; ^1H NMR (300 MHz, $CDCl_3$) δ 8.24 (s, 1H), 7.48–7.56 (m, 5H), 7.39–7.44 (m, 3H), 7.26–7.29 (m, 1H), 5.32 (s, 2H), 2.92–3.05 (m, 2H), 2.52–2.77 (m, 2H); $^{13}C\{^1H\}$ NMR (75 MHz, $CDCl_3$+DMSO-d_6) δ 158.1, 152.1, 148.8, 144.1, 142.1, 137.9, 135.4,

131.0, 130.7, 128.8, 128.4, 126.8, 126.2, 122.3, 118.8, 118.3, 115.7, 112.2, 23.9, 20.3. HRMS (ESI-TOF) m/z: $[M + H]^+$ Calcd for $C_{23}H_{17}ClN_5$ 398.1172; Found 398.1161.

2-Amino-4-(3-nitrophenyl)-7-diphenyl-6,7-dihydro-5H-pyrazolo[3,4-h]quinoline-3-carbonitrile **5d**. Obtained as yellow solid; Yield: 0.173 g, 90%; m.p.: 179–181 °C; IR ν: 3316, 2203, 1737, 1524, 1502 cm^{-1}; ^1H NMR (300 MHz, $CDCl_3$) δ 8.34–8.38 (m, 1H), 8.21 (s, 1H), 7.63–7.88 (m, 2H), 7.45–7.59 (m, 5H), 7.40–7.44 (m, 1H), 5.25 (s, 2H), 2.94–3.00 (m, 2H), 2.65–2.80 (m, 2H); $^{13}C\{^1H\}$ NMR (75 MHz, $CDCl_3$+DMSO-d_6) δ 164.6, 158.6, 154.8, 153.4, 148.2, 144.1, 143.3, 142.6, 140.2, 135.5, 134.6, 133.0, 129.0, 128.6, 128.4 125.1, 122.1, 120.4, 92.0, 30.3, 26.5. HRMS (ESI-TOF) m/z: $[M + H]^+$ Calcd for $C_{23}H_{17}N_6O_2$ 409.1413; Found 409.1418.

2-Amino-4-(naphthyl)-7-diphenyl-6,7-dihydro-5H-pyrazolo[3,4-h]quinoline-3-carbonitrile **5e**. Obtained as yellow solid; Yield: 0.171 g, 88%; m.p.: 190–193 °C; IR ν: 3342, 2212, 1738, 1556, 1503 cm^{-1}; ^1H NMR (300 MHz, $CDCl_3$) δ 8.27 (s, 1H), 7.96 (m, 2H), 7.31–7.78 (m, 10H), 5.31 (s, 2H), 2.84 (t, *J*=6.0 Hz, 2H), 2.50 (t, *J*=6.0 Hz, 2H); $^{13}C\{^1H\}$ NMR (75 MHz, $CDCl_3$+ DMSO-d_6) δ 158.0, 151.3, 149.4, 141.5, 137.4, 135.9, 132.7, 131.9, 129.0, 127.7, 127.1, 126.6, 125.5, 124.9, 124.1, 123.2, 121.7, 118.5, 115.5, 115.1, 86.8, 23.52, 19.76. HRMS (ESI-TOF) m/z: $[M + H]^+$ Calcd for $C_{27}H_{20}N_5$ 414.1719; Found 414.1719.

2-Amino-4-(2,4-dicholorophenyl)-7-diphenyl-6,7-dihydro-5H-pyrazolo[3,4-h]quinoline-3-carbonitrile **5f**. Obtained as yellow solid; Yield: 0.183 g, 90%; m.p.: 266–269 °C; IR ν: 3222, 2923, 2213, 1738, 1550, 1503 cm^{-1}; ^1H NMR (300 MHz, $CDCl_3$) δ 8.19 (s, 1H), 7.40–7.57 (m, 6H), 7.22–7.27 (m, 3H), 5.20 (s, 2H), 2.90–3.03 (m, 2H), 2.65–2.70 (m,1H), 2.54–2.61 (m,1H); $^{13}C\{^1H\}$ NMR (75 MHz, DMSO) δ 160.1, 153.7, 149.2, 144.3, 139.5, 137.8, 135.4, 135.1, 133.5,

132.5, 130.2, 130.1, 128.9, 128.5, 124.0, 120.2, 117.3, 116.0, 87.0, 80.2, 79.8, 79.4, 25.3, 21.5. HRMS (ESI-TOF) m/z: $[M + H]^+$ Calcd for $C_{23}H_{16}Cl_2N_5$ 432.0783; Found 432.0801.

2-Amino-4,7-bis-(4-cholorophenyl)-6,7-dihydro-5H-pyrazolo[3,4-h]quinoline-3-carbonitrile **5g**. Obtained as pale yellow solid; Yield: 0.193 g, 95%; m.p.: 201–203 °C; IR ν: 3318, 2203, 1735, 1550, 1495 cm^{-1}; ^1H NMR (300 MHz, $CDCl_3$) δ 8.19 (s, 1H), 7.36–7.57 (m, 6H), 7.18–7.33 (m, 3H), 5.21 (s, 2H), 2.92 (t, *J* =6.0 Hz, 2H), 2.75 (t, *J* = 6.0 Hz, 2H); $^{13}C\{^1H\}$ NMR (75 MHz, $CDCl_3$+DMSO-d_6) δ170.0, 165.0, 164.9, 159.1, 158.0, 156.7, 156.3, 150.0, 148.3, 147.3, 142.8, 135.5, 134.7, 134.1, 129.8, 120.3, 92.4, 30.2, 26.5. HRMS (ESI-TOF) m/z: $[M + H]^+$ Calcd for $C_{23}H_{16}Cl_2N_5$ 432.0783; Found 432.0790.

2-Amino-7-(4-chlorophenyl)-4-(4-methoxyphenyl)-6,7-dihydro-5H-pyrazolo[3,4-h]quinoline-3-carbonitrile **5h.** Obtained as brown solid; Yield: 0.156 g, 90%; m.p.: 200–203 °C; IR ν: 3331, 2205, 1609, 1555, 1514 cm^{-1}; ^1H NMR (400 MHz, DMSO) δ 8.12 (s, 1H), 7.57 (d, *J* = 12.0 Hz, 2H), 7.48 (s, 3H), 7.26 (d, *J* = 8.0 Hz, 2H), 7.02 (d, *J* = 8.0 Hz, 2H), 5.70 (s, 2H), 3.87 (s, 3H), 2.80–2.77 (m, 2H), 2.61 (d, *J* = 12.0 Hz, 2H); $^{13}C\{^1H\}$ NMR (100 MHz, DMSO) δ 152.7, 152.4, 142.8, 137.8, 137.5, 133.2, 129.8, 129.4, 128.4, 124.4, 120.4, 117.5, 115.9, 114.1, 88.3, 55.3, 25.1, 21.4. HRMS (ESI-TOF) m/z: $[M + H]^+$ Calcd for $C_{24}H_{19}ClN_5O$ 428.1200; Found 428.2500.

2-Amino-4-(4-methoxyphenyl)-7-(p-tolyl)-6,7-dihydro-5H-pyrazolo[3,4-h]quinoline-3-carbonitrile **5i.** Obtained as brown solid; Yield: 0.165 g, 92%; m.p.: 195–198 °C IR ν: 3323, 3214, 2202, 1625, 1609 cm^{-1}; ^1H NMR (400 MHz, $CDCl_3$) δ 8.14 (s, 1H), 7.35 (s, 3H), 7.30–7.25 (m, 4H), 7.02 (d, *J* = 8.0 Hz, 2H), 5.36 (s, 2H), 3.87 (s, 3H), 2.92–2.88 (m, 2H), 2.78 (d, *J* = 8.0 Hz, 2H), 2.41 (s, 3H); $^{13}C\{^1H\}$ NMR (100 MHz, $CDCl_3$) δ 159.7, 158.6, 152.1, 142.1, 137.5, 137.1, 136.2, 129.6, 129.5, 128.1, 122.9, 119.6, 117.30, 116.1, 113.8, 88.0, 55.1, 25.0, 21.1, 20.8. HRMS (ESI-TOF) m/z: $[M + H]^+$ Calcd for $C_{25}H_{22}N_5O$ 408.1746; Found 408.2177.

Ethyl-2-amino-4-(4-cholorophenyl)-7-phenyl-6,7-dihydro-5H-pyrazolo[3,4-h]quinoline-3-carboxalate **5j.** Obtained as yellow solid; Yield: 0.096 g, 46%; m.p.: 214–217 °C; IR ν: 3321, 3213, 2921, 2202, 1736 cm^{-1}; ^1H NMR (400 MHz, $CDCl_3$) δ 8.20 (s, 1H), 7.49 (d, *J* = 4.0 Hz, 4H), 7.38 (d, *J* = 8.0 Hz, 3H), 7.08 (d, *J* = 8.0 Hz, 2H), 6.14 (s, 2H), 3.89–3.85 (m, 2H), 2.90 (t, *J* = 8.0 Hz, 21H), 2.57 (t, *J* = 8.0 Hz, 2H), 0.76 (t, *J* = 8.0 Hz, 3H); $^{13}C\{^1H\}$ NMR (100 MHz, $CDCl_3$) δ 168.1, 158.1, 152.2, 150.0, 142.5, 139.0, 137.5, 133.0, 129.2, 129.1, 128.2, 127.5, 123.2, 120.1, 116.4, 104.4, 60.4, 29.7, 25.4, 21.6, 13.2. HRMS (ESI-TOF) m/z: $[M + H]^+$ Calcd for $C_{25}H_{22}ClN_2O_2$ 445.1353; Found 445.2898.

4-(4-Chlorophenyl)-2-oxo-7-phenyl-2,5,6,7-tetrahydro-1H-pyrazolo[3,4-h]quinoline-3-carbonitrile **5k.** Obtained as yellow solid; Yield: 0.094 g, 50%; m.p.: 203–206 °C; IR ν: 3327, 2921, 2205, 1625, 1610 cm^{-1}; ^1H NMR (400 MHz, $CDCl_3$) δ 14.71 (s, 1H), 8.67 (s, 1H), 7.50 (d, *J* = 8.0 Hz, 3H), 7.41 (d, *J* = 8.0 Hz, 2H), 7.17 (d, *J* = 8.0 Hz, 2H), 6.95 (s, 2H), 3.00 (s, 2H), 2.56 (s, 2H); $^{13}C\{^1H\}$ NMR (100 MHz, $CDCl_3$) δ 162.9, 159.5, 144.6, 143.8, 138.5, 137.8, 135.0, 133.6, 129.5, 129.4, 128.6, 128.2, 123.8, 113.6, 110.1, 97.7, 24.6, 21.1. HRMS (ESI-TOF) m/z: $[M + H]^+$ Calcd for $C_{23}H_{16}ClN_4O$ 399.0934; Found 397.2457

ASSOCIATED CONTENT

Supporting Information

The Supporting Information is available free of charge on the ACS Publications website at DOI: NMR, IR and HRMS of all the new products, log file of theoretical calculations and X-ray data for **5a** (CIF).

AUTHOR INFORMATION

Corresponding Author

*E-mail: raju.ranjithkumar@gmail.com

ORCID

Raju Ranjith Kumar: 0000-0002-9926-7770

ACKNOWLEDGEMENTS

RRK, AS and SSR thank the DST, New Delhi for funds under IRHPA program for the high resolution NMR facility in the Department and the DST-PURSE program, MKU. AS thanks DST, New Delhi for the INSPIRE fellowship (IF160126). The authors thank Prof. S. Murugesan and Dr. A. Siva, Department of Inorganic Chemistry, School of Chemistry, Madurai Kamaraj University for UV and emission studies and the theoretical calculations. The authors thank Dr. S. Easwaramoorthi, CLRI, Chennai, for the fluorescence lifetime measurements.

REFERENCES

1. Nayab, P. S.; Shkir, M. A Dual Responsive Colorimetric and Fluorescent Reversible Turn-On Chemosensor for Iron (Fe^{3+}): Computational and Spectroscopic Investigations. *Sens. Actuator B Chem*. **2017**, *245*, 395.
2. Yang, Z.; She, M.; Yin, B.; Cui, J.; Zhang, Y.; Sun, W.; Li, J.; Shi, Z. Three Rhodamine-Based "Off-On" Chemosensors with High Selectivity and Sensitivity for Fe^{3+} Imaging in Living Cells. *J. Org. Chem.* **2012**, *77*, 1143.

3. Hayashi, T.; Osawa, A.; Watanabe, T.; Murata, Y.; Nakayama, A.; Namba, K. Development of 1,3a,6a-Triazapentalene-Labeled Enterobactin as a Fluorescence Quenching Sensor of Iron Ion. *Tetrahedron Lett.* **2017**, *58*, 1961.
4. Sahoo, S. K.; Sharma, D.; Bera, R. K.; Crisponi, G.; Callan, J. F. Iron(III) Selective Molecular and Supramolecular Fluorescent Probes.*Chem. Soc. Rev.* **2012,** *41*, 7195.
5. Zhao, L.; Xin, X.; Ding, P.; Song, A.; Xie, Z.; Shen, J.; Xu, G. Fluorescent Oligomer as a Chemosensor for the Label-Free Detection of Fe^{3+} and Dopamine with Selectivity and Sensitivity. *Anal. Chim. Acta*. **2016**, 926, 99.
6. Jiang, J.; Gao, P.; Zhang, Y.; Zhang, G.; Zhou, Y.; Dong, C.; Shuang, S. Rapid One-Pot Synthesis of MMTA Protected Fluorescent Gold Nanoclusters for Selective and Sensitive Detection of Ferric ion. *Talanta.* **2017**, *174*, 44.
7. En, D.; Guo, Y.; Chen, B.T.; Dong, B.; Peng, M. J. Coumarin-Derived Fe^{3+} Selective Fluorescent Turn-Off Chemosensors: Synthesis, Properties, and Applications in Living Cells. *RSC Adv.* **2014**, *4*, 248.
8. Swain, R.; Sahoo, B. Mapping of Heavy Metal Pollution in River Water at Daily Time-Scale Using Spatio-Temporal Fusion of MODIS-Aqua and Landsat Satellite Imageries. *J. Environ. Manage.* **2017**, *192*, 1.
9. (a) Wu, D.; Sedgwick, A. C.; Gunnlaugsson, T.; Akkaya, E. U.; Yoon, J.; James, T. D. Fluorescent Chemosensors: the Past, Present and Future. *Chem*. *Soc*. *Rev*. **2017**, *46*, 7105; (b) *Fluorescent Chemosensors for Ion and Molecule Recognition*; Czarnik, A. W., Eds.; ACS Symposium Series 538; American Chemical Society: Washington, DC, 1993.

10. Yang, Y.; Wang, X.; Cui, Q.; Cao, Q.; Li, L. Self-Assembly of Fluorescent Organic Nanoparticles for Iron(III)Sensing and Cellular Imaging.*ACS Appl. Mater. Interfaces.* **2016**, *8*, 7440.
11. Basoglu, A.; Tosun, G.; Ocak, M.; Alp, H.; Yaylı, N.; Ocak, U. Simple Time-Saving Method for Iron Determination Based on Fluorescence Quenching of an Azaflavanon-3-ol Compound. *J. Agric. Food Chem.* **2015**, *63*, 2654.
12. Xu, H.; Ding, H.; Li, G.; Fan, C.; Liu, G.; Pu, S. A Highly Selective Fluorescent Chemosensor for Fe^{3+} Based on a New Diarylethene with a Rhodamine 6G Unit. *RSC Adv*. **2017**, *7*, 29827.
13. Garcia-Beltran, O.; Cassels, B.; Perez, C.; Mena, N.; Nunez, M.; Martinez, N.; Pavez, P.; Aliaga, M. Coumarin-Based Fluorescent Probes for Dual Recognition of Copper(II) and Iron(III) Ions and Their Application in Bio-Imaging. *Sensors.* **2014**, *14*, 1358.
14. Pan, C.; Wang, K.; Ji, S.; Wang, H.; Li, Z.; He, H.; Huo, Y. Schiff Base Derived Fe^{3+}-Selective Fluorescence Turn-Off Chemosensors Based on Triphenylamine and Indole: Synthesis, Properties and Application in Living Cells. *RSC Adv.* **2017**, *7*, 36007.
15. Li, P.; Zhang, M.; Sun, X.; Guan, S.; Guang, Z.; Baumgarten, M.; Mullen, K. A Dendrimer-Based Highly Sensitive and Selective Fluorescence Quenching Sensor for Fe^{3+} both in Solution and as Film. *Biosens. Bioelectron.* **2016**, *85*, 785.
16. Koner, R.R.; Sinha, S.; Kumar, S.; Nandi, C.K.; Ghosh, S. 2-Aminopyridine Derivative as Fluorescence 'On–Off' Molecular Switch for Selective Detection of $Fe^{3+/}Hg^{2+}$. *Tetrahedron Lett.* **2012**, *53*, 2302.

17. Huang, L.; Hou, F.; Cheng, J.; Xi, P.; Chen, F.; Bai, D.; Zeng, Z. Selective Off–On Fluorescent Chemosensor for Detection of Fe^{3+} ions in Aqueous Media. *Org. Biomol. Chem.* **2012**, *10,* 9634.

18. Nandre, J.; Patil, S.; Patil, V.; Yu, F.; Chen, L.; Sahoo, S.; Prior, T.; Redshaw, C.; Mahulikar, P.; Patil, U. A Novel Fluorescent "Turn-On" Chemosensor for Nanomolar Detection of Fe(III) From Aqueous Solution and Its Application in Living Cells Imaging. *Biosens. Bioelectron.* **2014**, *61*, 612.

19. Yang, W.; Cheng, Z.; Xu, Y.; Shao, J.; Zhou, W.; Xie, J.; Li, M. A Highly Selective Fluorescent Chemosensor for Cyanide Anions Based on a Chalcone Derivative in the Presence of Iron(III) Ions, and Its Capacity for Living Cell Imaging in Mixed Aqueous Systems. *New J. Chem.,* **2015**, *39*, 7488.

20. Zhou, F.; Leng, T-H.; Liu, Y-J.; Wang, C-Y.; Shi, P.; Zhu, W-H. Water-Soluble Rhodamine-Based Chemosensor for Fe3+ with High Sensitivity, Selectivity and Anti-interference Capacity and its Imaging Application in Living Cell. *Dyes and Pigments* **2017**, *142*, 429.

21. Li, G.; Tang, T.; Ding, P.; Ye, T. A Rhodamine-Benzimidazole Based Chemosensor for Fe(3+) and its Application in Living Cell. *J. Fluoresc*. **2015**, *26*, 155.

22. Li, S.; Zhang, D.; Xie, X.; Ma, S.; Liu, Y.; Xu, Z.; Gao, Y.; Ye, Y. A Novel Solvent-Dependently Bifunctional NIR Absorptive and Fluorescent Ratiometric Probe for Detecting Fe^{3+}/Cu^{2+} and its Application in Bioimaging. *Sens. Actuator B Chem*. **2016**, *224*, 661.

23. Gaurav, A.; Gautam, V.; Singh, R. An Overview on Synthetic Methodologies and Biological Activities of Pyrazoloquinolines. *Mini Rev*. *Med*. *Chem*. **2010**, *10*, 1194.

24. (a) Tao, Y. T.; Balasubramaniam, E.; Danel, A.; Wisla, A.; Tomasik, P. Pyrazoloquinoline Derivatives as Efficient Blue Electroluminescent Materials. *J. Mater. Chem.* **2001**, *11*, 768; (b) Gondek, E.; Kityk, I. V.; Danel, A. Molecular Engineering by Light Emitting Diode Parameters on the Base of Methoxy-Pyrazoloquinoline Dyes in Polysilane Matrices. *J. Phys. D: Appl. Phys.* **2007**, *40,* 2748; (c) Rechthaler, K.; Rotkiewicz, K.; Danel, A.; Tomasik, P.; Khatchatryan, K.; Kohler, G. Emissive Properties and Intramolecular Charge Transfer of Pyrazoloquinoline Derivatives. *J. Fluoresc.* **1997**, *7*, 301; (d) Gondek, E.; Kityk, I. V.; Sanetra, J.; Szlachcic, P.; Armatys, P.; Wisla, A.; Danel, A. New-Synthesized Pyrazoloquinoline as Promising Luminescent Materials. *Opt. Laser Technol.* **2006**, *38,* 487.; (e) Gondek, E.; Danel,; Kityk, I. V. Single-Layered Light-Emitting Diodes Possessing Methoxy-Modified Pyrazoloquinoline Dyes in Poly-N-vinylcarbazole Matrix. *J. Lumin.* **2008**, *128,* 348; (f) Danel, A.; Chacaga, L.; Uchacz, T.; Pokladko-Kowar, M.; Gindek, E.; Karasinski, P.; Sahraoui, B. Solution Processable Double Layer Organic Light Emitting Diodes (OLEDs) Based on 6-N,N-Arylsubstituted-1H-Pyrazolo[3,4-b]Quinolines. *Advanced Device Materials*, **2015**, *1*, 17; (g) Mac, M.; Uchacz, T.; Danel, A.; Musiolik, H. Applications of Fluorescent Sensor Based on 1H-Pyrazolo[3,4-b]Quinoline in Analytical Chemistry. *J. Fluoresc.* **2013**, *23,* 1207; (h) Rurack, K.; Danel, A.; Rotkiewicz, K.; Grabka, D.; Spieles, M.; Rettig, W. 1,3-Diphenyl-1H-Pyrazolo[3,4-b]Quinoline: A Versatile Fluorophore for the Design of Brightly Emissive Molecular Sensors. *Org. Lett.,* **2002**, 4, *26*, 4647; (i) Gayathri, K.; Velmurugan. K.; Nandhakumar, R.; Malathi, M.; Madhusalini,S.; Mohan, P.S.; Shankar,R. New Pyrazolo-Quinoline Scaffold as a Reversible Colorimetric Fluorescent

Probe for Selective Detection of Zn^{2+} Ions and Its Imaging in Live Cells. *J. Photochem. Photobiol,. A: Chem*, **2017**, *341*, 136.

25. (a) Kaplan, A. P.; Gupta, V.; Wasley, J. W. F. US Patent US7872002B2, 2007; (b) Kasaboina, S.; Ramineni, V.; Banu, S.; Bandi, Y.; Nagarapu, L.; Dumala, N.; Grover, P. Iodine Mediated Pyrazolo-Quinoline Derivatives as Potent Anti-Proliferative Agents *Bioorg. Med. Chem. Lett.* **2018**, *28*, 664; (c) Yang, S-W.; Smotryski, J.; McElroy, W. T.; Tan, Z.; Ho, G.; Tulshian, D.; Greenlee, W. J.; Guzzi, M.; Zhang, X.; Mullins, D.; Xiao, L.; Hruza, A.; Chan, T-M.; Rindgen, D.; Bleickardt, C.; Hodgson, R. Discovery of Orally Active Pyrazoloquinolines as Potent PDE10 Inhibitors for the Management of Schizophrenia. *Bioorg. Med. Chem. Lett.* **2012**, *22*, 235; (d) Bekhit, A. A.; El-Sayed, O. A.; Aboul-Enein, H. Y.; Siddiqui, Y. M.; Al-Ahdal, M. N.; Effect of Pyrazoloquinoline Derivatives on the Growth of Leishmania Donovani Promastigotes. *Arch. Pharm. Pharm. Med. Chem.* **2005**, *338*, 74; (d) Lee, C. S.; Allwine, D. A.; Barbachyn, M. R.; Grega, K. C.; Dolak, L. A.; Ford, C. W.; Jensen, R. M. et al., Carbon–Carbon-Linked (Pyrazolylphenyl)oxazolidinones with Antibacterial Activity Against Multiple Drug Resistant Gram-Positive and Fastidious Gram-Negative Bacteria. *Bioorg. Med. Chem.* **2001**, *9,* 3243; (e) Baraldi, P. G.; Pavani, M. G. M.; Nunez, G. M. C.; Brigidi, P.; Vitali, B.; Gambari, R.; Romagnoli, R.; Antimicrobial and Antitumor Activity of N-Heteroimmine-1,2,3-dithiazoles and Their Transformation in Triazolo-, Imidazo-, and Pyrazolopyrimidines. *Bioorg. Med. Chem.* **2002**, *10,* 449; (f) (g).

26. (a) Colotta, V.; Catarzi, D.; Varano, F.; Cecchi, L.; Filacchioni, G.; Martini, C.; Trincavelli, L.; Lucacchini, A. Synthesis and Structure-Activity Relationships of a New Set of 2-Arylpyrazolo[3,4-c]Quinoline Derivatives as Adenosine Receptor Antagonists.

J. Med. Chem. **2000,** *43,* 3118; (b) Tu , S.; Wu, S.; Zhang, X.; Han, Z.; Cao, X.; Hao, W. One-Step Efficient Synthesis of Pyrazolo[3,4-f]quinoline Derivatives Under Microwave Irradiation. *Synth. Commun. 40,* **2010**, 1057; (c) Chaczatrian, K.; Chaczatrian, G.; Danel, A.; Tomasik, P. The Synthesis of 4-Aryl-1H-Pyrazolo[3,4-b]Quinolines by Cyclization of 4-Arylidenepyrazolin-5-Ones with Anilines. *ARKIVOC.* **2001**, *6,* 63; (d) Ghotekar, B. K.; Jachak, M. N.; Toche, R. B. New One-Step Synthesis of Pyrazolo[1,5-a]pyrimidine and Pyrazolo[1,5-a]Quinazoline Derivatives via Multicomponent Reactions *J. Heterocyclic Chem.* **2009**, *46*, 708. (e) Quiroga, J.; Portillo, S.; Perez, A.; Galvez, Abonia, J. R.; Insuasty, B. An Efficient Synthesis of Pyrazolo[3,4-b]Pyridine-4-Spiroindolinones by a Three-Component Reaction of 5-Aminopyrazoles, Isatin, and Cyclic β-Diketones. *Tetrahedron Lett.* **2011,** *52,* 2664.

27. Spano, V.; Parrino, B.; Carbone, A.; Montalbano, A.; Salvador, A.; Burn, P.; Vedaldi, D.; Diana, P.; Cirrincione, G.; Barraja, P. Pyrazolo[3,4-h]Quinolines Promising Photosensitizing Agents in the Treatment of Cancer. *Eur. J. Med. Chem*. **2015**, *102*, 334.
28. (a) Tietze, L. F.; Brasche, G.; Gericke, K. M. In Domino Reactions in Organic Synthesis Wiley-VCH: Weinheim, **2006**; (b) Tietze, L. F.; (Ed.) Domino Reactions: Concepts for Efficient Organic Synthesis, Wiley-VCH, Weinheim, **2014**.
29. (a) Lidstrom, P.; Tierney, J.; Wathey, B.; Westman, J. Microwave Assisted Organic Synthesis- a Review. *Tetrahedron* **2001**, *57*, 9225; (b) Caddick, S. Microwave Assisted Organic Reactions. *Tetrahedron.* **1995**, *51,* 10403; (c) Bogdal, Microwave-Assisted Organic Synthesis, Volume 25, Elsevier Science, **2005**.
30. (a) Tu, S-J.; Jiang, B. Microwave-Assisted Domino Reaction in Organic Synthesis, Ed. Grundas, S. Intech Open Limited, UK, **2011**, p 673; (b) Gawande, M. B.; Shelke, S. N.;

Zboril, R.; Varma, R. S. Microwave-Assisted Chemistry: Synthetic Applications for Rapid Assembly of Nanomaterials and Organics *Acc. Chem. Res.,* **2014**, *47*, 1338; (c) Presset, M.; Coquerel, Y.; Rodriguez, *J.* Microwave-Assisted Domino and Multicomponent Reactions with Cyclic Acylketenes: Expeditious Syntheses of Oxazinones and Oxazindiones. *Org. Lett.,* **2009**, *11*, 5706.

31. Molteni, V.; Hamilton, M. M.; Mao, L.; Crane, C. M.; Termin, A. P.; Wilson, D. M. Aqueous One-Pot Synthesis of Pyrazoles, Pyrimidines and Isoxazole Promoted by Microwave Irradiation. *Synthesis*, **2002**, *12*, 1669.
32. Crystallographic Data for Compound **5b** has been deposited with the Cambridge Crystallographic Data Center as Supplementary Publication Number CCDC 1837442.
33. (a) Melhuish, W.H. Quantum Efficiencies of Fluorescence of Organic Substances: Effect of Solvent and Concentration of the Fluorescent Solute. *J. Phys. Chem.,* **1961**, 65, 229; (b) Williams, A.T.R.; Winfield, S.A. Relative Fluorescence Quantum Yields Using a Computer-Controlled Luminescence Spectrometer. *Analyst,* **1983**, 108, 1067-1071; (c) The relative quantum yield of compounds **5a–g** was calculated using the following equation

$$\Phi_S = \Phi_{ST} (Grad_S/Grad_{ST})(\eta^2_S/\eta^2_{ST})$$

where Φ_S and Φ_{ST} denotes quantum yield of sample and standard respectively, *Grad* represents the gradient from the plot of integrated fluorescence intensity *vs* absorbance, η_S and η_{ST} represents the refractive index of the sample and standard respectively.

34. Liu, Y.; Xu, Z.; Wang, J.; Zhang, D.; Ye, Y.; Zhao, Y. Two New Rhodamine-Based Fluorescent Chemosensors for Fe^{3+} in Aqueous Solution. *Luminescence*, **2014**, *29*, 945.

35. Chen, W.; Gong, W.; Ye, Z.; Lina, Y.; Ning, G. FRET-Based Ratiometric Fluorescent Probes for Selective Fe^{3+} Sensing and Their Applications in Mitochondria. *Dalton Trans.,* **2013**, *42*, 10093.

36. Mao, J.; Wang, L.; Dou, W.; Tang, X.; Yan, Y.; Liu, W. Tuning the Selectivity of Two Chemosensors to Fe(III) and Cr(III). *Org. Lett.,* **2007**, 9, *22*, 4567.

37. Chen, X.; Hong, H.; Han, R.; Zhang, D.; Ye, Y.; Zhao, Y. A New bis(rhodamine)-Based Fluorescent Chemosensor for Fe^{3+}. *J. Fluoresc*., **2012**, *22*, 789.

38. Yang, Y.; Wang, X.; Cui, Q.; Cao, Q.; Li, L. Self-Assembly of Fluorescent Organic Nanoparticles for Iron(III)Sensing and Cellular Imaging. *ACS Appl. Mater. Interfaces* **2016**, 8, 7440.

39. Fox, D. J. Gaussian 09, Revision A. 02, Gaussian, Inc, Wallingford, CT, 2009.

TOC Graphics